

Article

# The Study on the Cultivable Microbiome of the Aquatic Fern *Azolla Filiculoides* L. as New Source of Beneficial Microorganisms

Artur Banach <sup>1,\*</sup>, Agnieszka Kuźniar <sup>1</sup>, Radosław Mencfel <sup>2</sup> and Agnieszka Wolińska <sup>1</sup>

<sup>1</sup> Department of Biochemistry and Environmental Chemistry, The John Paul II Catholic University of Lublin, 20-708 Lublin, Poland; agawoloszyn@kul.pl (A.K.); awolin@kul.pl (A.W.)

<sup>2</sup> Department of Animal Physiology and Toxicology, The John Paul II Catholic University of Lublin, 20-708 Lublin, Poland; mencfelr@kul.pl

\* Correspondence: abanach@kul.pl; Tel.: +48-81-454-5442

Received: 6 May 2019; Accepted: 24 May 2019; Published: 26 May 2019



**Abstract:** The aim of the study was to determine the still not completely described microbiome associated with the aquatic fern *Azolla filiculoides*. During the experiment, 58 microbial isolates (43 epiphytes and 15 endophytes) with different morphologies were obtained. We successfully identified 85% of microorganisms and assigned them to 9 bacterial genera: *Achromobacter*, *Bacillus*, *Microbacterium*, *Delftia*, *Agrobacterium*, and *Alcaligenes* (epiphytes) as well as *Bacillus*, *Staphylococcus*, *Micrococcus*, and *Acinetobacter* (endophytes). We also studied an *A. filiculoides* cyanobiont originally classified as *Anabaena azollae*; however, the analysis of its morphological traits suggests that this should be renamed as *Trichormus azollae*. Finally, the potential of the representatives of the identified microbial genera to synthesize plant growth-promoting substances such as indole-3-acetic acid (IAA), cellulase and protease enzymes, siderophores and phosphorus (P) and their potential of utilization thereof were checked. *Delftia* sp. AzoEpi7 was the only one from all the identified genera exhibiting the ability to synthesize all the studied growth promoters; thus, it was recommended as the most beneficial bacteria in the studied microbiome. The other three potentially advantageous isolates (*Micrococcus* sp. AzoEndo14, *Agrobacterium* sp. AzoEpi25 and *Bacillus* sp. AzoEndo3) displayed 5 parameters: IAA (excluding *Bacillus* sp. AzoEndo3), cellulase, protease, siderophores (excluding *Micrococcus* sp. AzoEndo14), as well as mineralization and solubilization of P (excluding *Agrobacterium* sp. AzoEpi25).

**Keywords:** *Azolla*; *Delftia* sp., endophytes; plant growth promoting potential; *Trichormus azollae*

## 1. Introduction

Plants and microorganisms form complex associations displaying diverse interactions ranging from mutualism to pathogenicity. The habitat for microorganisms can be both the interior (endosphere occupied by endophytes) and the surroundings (phyllosphere, rhizoplane, and rhizosphere occupied by epiphytes) of the host plant [1,2]. Microbial genomes, referred to as the microbiome or plants' second genome [2,3], constitute a specific plant microbiome together with the plant genome. Additionally, given the co-evolution process between plants and their associated microbiome resulting in a strong genomic interdependency, plants and their microbiome are considered as a metaorganism or a holobiont [4].

Plant-associated microbes, especially endophytes, play a crucial role in plant growth and development, allowing them to survive harsh conditions [1], which is important for food production (increased crops, biocontrol of plant diseases) and for coping with contaminants (phytoremediation). These beneficial microorganisms are termed as Plant Growth-Promoting Bacteria (PGPB) [3,5].

Their beneficial function is the improvement of plant fitness and protection against biotic and abiotic stresses by facilitation of nutrient acquisition and providing plant hormones and other metabolites [3,6]. The presence of pollutants, such as heavy metals, may also pose a threat to both plants and some microorganisms (e.g., metal-tolerant species); however, they may be able to immobilize or decompose pollutants, thus protecting plants or improving their defense mechanisms. This issue is crucial for bioremediation and phytoremediation processes [7,8].

Despite the enormous microbial abundance in different environments and the substantial progress in their cultivation methods, still only 1% of these microorganisms can be cultured [9]. In addition, some endophytes are commensals with a yet unknown function in plants. It is also very common to study the function of the microbiome for a specific group of species and to focus mostly on terrestrial plants rather than on a broader taxonomical spectrum of plant species [3]. Therefore, it is worth discovering microbiomes associated with plants providing new microbiomes that can potentially be valuable to humans. Valuable plants in terms of potential microbiome hosts are ferns belonging to the genus *Azolla*, which play important roles in some branches of industry [10,11].

*Azolla filiculoides* L. (*Salviniaceae*) is a small (2.5 cm) heterosporous floating aquatic or semiaquatic pteridophyte occurring on the surface of eutrophic waters in temperate and tropical climate around the world (Figure 1a). It can exist either individually or in mats, which can reach a thickness of up to 20 cm. The fern has bilobed leaves. The dorsal lobe has an ovoid cavity inhabited by the community of cyanobacteria *Anabaena azollae* (Starr) (Figure 1b) capable of atmospheric nitrogen fixing using the nitrogenase enzyme (EC 1.18.6.1) in specialized thick-walled cells called heterocysts (Figure 1c).

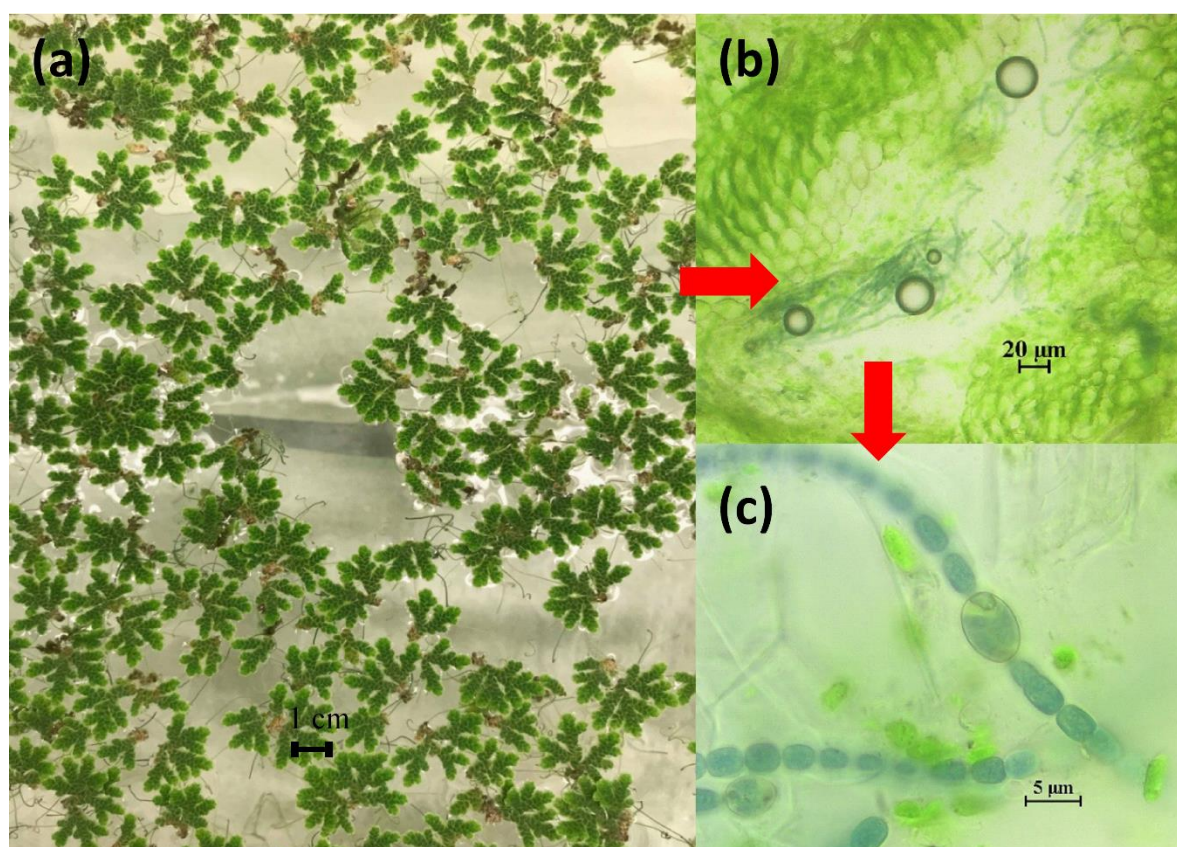


**Figure 1.** (a) Culture of *A. filiculoides* under laboratory conditions on IRRI medium; (b) filaments of *A. azollae* in a leaf cavity; (c) close up of *A. azollae*; both pictures taken from the light microscope at magnifications of 10x and 100x, respectively (Nikon Eclipse 80i, Nikon Instruments Europe B.V., Amsterdam, The Netherlands). Photo: A. Banach.

This trait makes *Azolla* sp. independent of other external nitrogen sources allowing its fast growth and production of high-protein biomass. Hence, *Azolla* sp. can be used as a green manure on rice fields and animal feed [10,11]. Another important feature of the fern is its capability of heavy metal accumulation [11,12].

Over the years, the cyanobiont has been named *Nostoc azollae*, *Anabaena azollae*, and *Trichormus azollae*, but no definitive classification exists to date. Studies by Plazinski et al. [13] suggested that the endosymbiont represents rather *Nostoc* sp. than *A. azollae*. Gebhardt and Nierzwicki-Bauer [14] reported that the classification of cyanobacteria depends on the host plant. In 2003, using comparisons of the sequences of the phycocyanin intergenic spacer and a fragment of the 16S rRNA, Baker and co-authors [15] found that the cyanobiont from *Azolla* sp. belongs to neither of these genera. In 2014, Pereira and Vasconcelos [16] made another attempt to solve this dilemma, but their results were also unclear. Consequently, the problem remains unsolved to date. There is some information about bacteria as a third partner in symbiosis. The presence of bacteria in *Azolla* sp. leaves was first reported by Grilli in 1964 [17] and microscopic observations thereof were done by Nierzwicki-Bauer and Aulfinger [18] and Carrapiço [19]. Serrano et al. [20] determined bacterial species accompanying *Azolla* sp. recognized in the 20th century. However, no more detailed analysis or identification of these bacteria has been performed.

All these issues are associated with a huge gap in knowledge on microorganisms inhabiting *Azolla* sp.; hence, our intention was to fill it. Thus, the novelty and main goal of the study was to isolate, identify, and describe unrecognized bacteria constituting the core microbiome of *A. filiculoides*. Since the fern is used in agriculture and water treatment, it would be useful to discover its microbiome, which may help to elucidate its role in the symbiotic system *Azolla*-microorganisms and indicate its possible applications in the branches of industry mentioned above.

## 2. Results

### 2.1. *Azolla* Cyanobiont

The isolation of the cyanobiont allowed us to observe the presence of dense agglomerations of cyanobiont filaments together with plant debris. After one week of cyanobiont culture, we collected sufficient amounts of living material for further studies; an example of the living culture is presented in Figure 2.

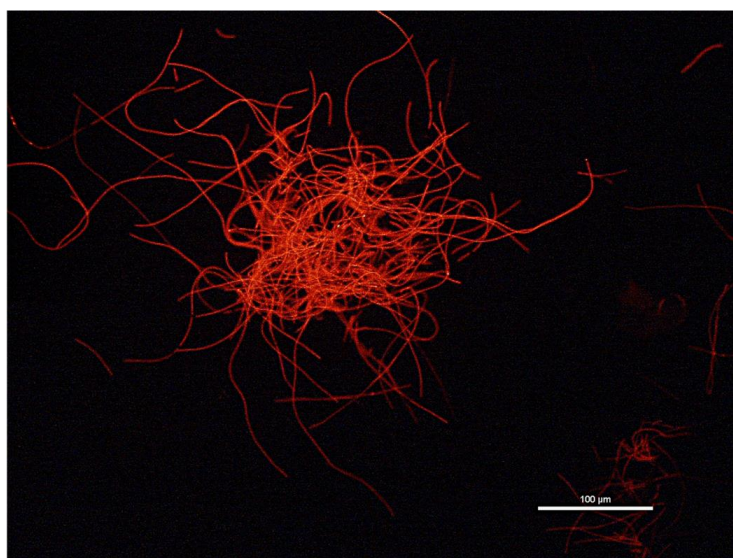


**Figure 2.** UV microphotograph of the cyanobiont culture obtained during passage (Nikon Eclipse 80i microscope, magnification 4x, UV2A filter, Nikon Instruments Europe B.V., Amsterdam, The Netherlands). Photo: A. Banach.

Colony filaments were not attenuated towards ends. Cells are ellipsoidal or barrel-shaped, size of cells changes from 4–6 × 2.5–3.5 µm, with granules. Heterocysts were ellipsoidal, larger than vegetative cells, size 5–9 × 4.5–6 µm, solitary and intercalary. Gas vacuoles were absent.

After conducting PCR reaction using *nifDf* and *nifDr* primers, specific products of 600 bp were obtained. This observation confirms the presence of the *nif* gene encoding enzymes important in atmospheric nitrogen fixing, i.e., a feature typical of cyanobacteria. In the case of primers targeting a fragment of the 16S rRNA gene specific for cyanobacteria, we obtained two 1500 and 1700 bp products specific for used primers [21]. After purification of the PCR products, the latter one was further analyzed.

The analysis of the similarity of the cyanobacterium-specific 16S rRNA gene fragments to a homologous gene revealed similarities to the previously described *Azolla* sp. cyanobionts (Table 1). We found four hits with a similarity of 90–94%, which indicates that the studied DNA fragments are likely to belong to *Anabaena* sp.

**Table 1.** Microorganisms similar to the homologous 16S rRNA gene specific for cyanobacteria (GenBank, NCBI).

Genus	Potential Microorganism	Similarity	Accession no.	Reference
<i>Anabaena</i>	<i>A. sp.</i> 6-HorLes10	94%	KT290350.1	[22]
	<i>A. sp.</i> HAN21/1	93%	KP701032.1	[23]
	<i>A. cf. cylindrica</i> 133	93%	AJ293110.1	[24]
	<i>A. oscillarioides</i> ORO34S1	90%	DQ264246.1	[25]

## 2.2. The Cultured Microbiome of *A. filiculoides*

The isolation yielded in 58 microbial isolates, among which 15 were obtained from the interior of the plant. We noticed differences in the morphology of the colonies, which suggests affiliation of the isolates to different taxonomic groups. The morphology of the obtained isolates is summarized in Table 2.

**Table 2.** Morphological traits of the isolates.

No.	Type	Size <sup>1</sup>	Form <sup>2</sup>	Surface <sup>3</sup>	Texture <sup>4</sup>	Opacity <sup>5</sup>	Pigmentation <sup>6</sup>	Elevation <sup>7</sup>	Margin <sup>8</sup>	Gram Staining
1		++	i	d/r	BUT	OPQ	cream	F	Ent	G-
2		++	i	g/r	BUT	OPQ	w-c	R	Und	G+
3		++	i	g/r	BUT	OPQ	cream	R	Und	G+
4		+	c	d/s	BRIT	OPQ	white	F	Ent	G+
5		++	c	d/s	BRIT	OPQ	white	F	Und	G+
6		++	i	d/s	BUT	OPQ	yel-c	F	Und	G+
7		.	c	g/s	BUT	TRANS	white	R	Ent	G-
8		.	c	g/r	BUT	TRANS	cream	R	Ent	G+
9		+	c	g/r	BUT	TRANS	yel-c	R	Ent	G+
10		+	c	g/r	BUT	TRANS	cream	R	Ent	G-
11	Epiphyte	++	i	d/r	BRIT	OPQ	yel-c	F	Und	G+
12		+	i	g/s	BUT	IRID	cream	C	Und	G-
13		+	c	g/s	BUT	OPQ	yel-c	U	Ent	G-
14		.	o	g/r	MUC	OPQ	cream	R	Ent	G-
15		+++	c	g/s	MUC	TRANS	yel-org	C	Ent	G-
16		++	c	d/s	BUT	OPQ	w-c	R	Ent	G+
17		++	o	d/s	BRIT	OPQ	w-c	F	Ent	G+
18		+	i	d/s	BUT	OPQ	cream	F	Und	G+
19		+++	o	d/s	BRIT	OPQ	cream	R	Und	G+
20		.	c	g/r	BUT	OPQ	cream	U	Ent	G-
21		+++	o	d/s	BUT	OPQ	beige	F	Und	G+
22		+++	c	d/r	BUT	OPQ	beige	R	Und	G+
23		+	c	g/s	BUT	TRANS	cream	R	Ent	G-
24		.	c	g/r	BUT	TRANS	beige	R	Ent	G-
25		.	o	g/s	MUC	TRANS	yellow	R	Ent	G+
26	.	o	g/s	MUC	TRANS	cream	R	Ent	G-	

Table 2. Cont.

No.	Type	Size <sup>1</sup>	Form <sup>2</sup>	Surface <sup>3</sup>	Texture <sup>4</sup>	Opacity <sup>5</sup>	Pigmentation <sup>6</sup>	Elevation <sup>7</sup>	Margin <sup>8</sup>	Gram Staining
27		+	c	g/s	BUT	TRANS	w-c	F	Und	G+
28		+	i	g/s	BUT	OPQ	yel-org	R	Und	G+
29		.	c	g/s	BUT	TRANS	cream	U	Ent	G-
30		+	c	g/r	BUT	OPQ	beige	R	Ent	G-
31		+	c	d/s	MUC	IRID	beige	U	Ent	G-
32		+	c	g/r	BUT	TRANS	beige	U	Ent	G-
33		.	c	g/r	BUT	TRANS	beige	U	Ent	G-
34		.	o	g/s	BUT	TRANS	cream	R	Ent	G-
35		++	o	d/r	BRIT	OPQ	cream	F	Ent	G+
36		.	c	g/s	BUT	TRANS	cream	U	Ent	G+
37		+++	f	g/s	BUT	TRANS	w-c	F	Fili	G+
38		.	c	g/s	MUC	OPQ	yellow	R	Ent	G+
39		+	c	g/s	MUC	TRANS	yellow	C	Ent	G-
40		+	i	g/r	BUT	OPQ	cream	U	Ent	G-
41		+	o	d/r	BUT	TRANS	cream	U	Ent	G+
42		+++	o	d/s	BRIT	TRANS	beige	F	Ent	G+
43		+++	o	d/s	BRIT	OPQ	beige	F	Und	G+
1	endophyte	.	c	g/r	BUT	OPQ	beige	U	Ent	G+
2		.	c	g/s	BUT	TRANS	cream	R	Ent	G+
3		.	c	g/s	BUT	OPQ	cream	R	Ent	G+
4		.	c	g/s	BUT	TRANS	w-c	R	Ent	G+
5		+	c	g/s	BUT	TRANS	w-c	R	Ent	G+
6		.	c	g/s	MUC	IRID	yellow	R	Ent	G+
7		.	c	g/s	BUT	IRID	yellow	R	Und	G+
8		.	c	g/s	MUC	OPQ	yellow	R	Ent	G+
9		+	c	g/s	BUT	OPQ	cream	R	Ent	G+
10		++	c	g/s	MUC	IRID	yellow	R	Ent	G+
11		++	c	g/s	MUC	OPQ	yellow	R	Ent	G+
12		+++	c	g/s	BUT	TRANS	cream	R	Ent	G+
13		++	c	g/s	BUT	OPQ	white-cream	R	Ent	G+
14		++	i	g/s	BUT	OPQ	white-cream	F	Und	G-
15		+	i	g/s	BUT	OPQ	white-cream	F	Und	G+

<sup>1</sup> —punctiform, +—small, ++—moderate, +++—large; <sup>2</sup> Form: o—oval, c—circular, i—irregular, f—filamentous, <sup>3</sup> d—dull, g—glistering, r—rough, s—smooth; <sup>4</sup> BUT—butyrous, MUC—mucoïd, BRIT—brittle, <sup>5</sup> OPQ—opaque, TRANS—translucent, IRID—iridescent; <sup>6</sup> w-c: White-cream, yel-c: Yellow-cream, yel-org: Yellow-orange; <sup>7</sup> F—flat, R—raised, C—convex, U—umbonate; <sup>8</sup> Ent—entire, Und—undulate, Fili—filiform.

The isolates displayed a wide range of colony sizes ranging from <1 mm to ca. 0.5 mm. More than 40% were both punctiform and small, above 20% were moderate in size, and the largest colonies constituted approximately 14%. The epiphytes showed the same pattern, whilst 46% of the endophytes were the smallest, 20% were small, 27% were moderate, and only ca. 7% had a large size.

The circular shape was dominant in the studied pool of microorganisms (60%), with substantially higher counts recorded for the endophytes (87%) than the epiphytes (51%). Oval and irregular shapes accounted for 19% of each of these shapes. Only one epiphytic isolate formed filamentous colonies (2%). The epiphytic microorganisms formed oval and irregular shapes in 26% and 21% cases as well. The endophytes did not form oval and filamentous colonies and an irregular form was recorded in 14% of these microorganisms.

In the case of surfaces, we distinguished dull-glistering and rough-smooth combinations. The glistering/smooth surface accounting for 50% of all isolates was the most abundant (35% and 93% of the epiphytes and endophytes, respectively). The next two abundant surfaces were glistering-rough (22%, 28%, and 6% for the total microbiome, epiphytes, and endophytes, respectively) and dull/smooth (19% of all microbes). The latter was present in 26% of epiphytes whilst endophytes displayed no such surface type. The dull/rough surface was the least common (8.6%); it was not observed for endophytes and only 12% of epiphytes were characterized by such a surface.

We observed three types of colony texture: Butyrous (BUT), mucoïd (MUC), and brittle (BRIT). The first type (BUT) was the most common in all microorganisms (67%) followed by MUC (19%) and BRIT (14%). A similar number was recorded for the epiphytes, whilst 73% of the endophytes had BUT and 27% MUC texture.

In terms of colony transparency, we divided the microorganisms into opaque (OPQ), translucent (TRANS), and iridescent (IRID). More than half or all microbes, both epi- and endophytes, produced non-transparent (OPQ) colonies whilst 40% were transparent (44% of epiphytes and 27% of endophytes). Opalescent color was observed in 9% of isolates (4.7% epi- and 20% of endophytes).

The isolated microorganisms displayed two types of pigmentation—white-cream-beige (76%) (Figure 3a) and yellow-orange (24%) (Figure 3b). Similar numbers were recorded for the epiphytes, whilst 2/3 of the endophytes were included in the “white group” and 1/3 in the “yellow group”. Deeper analysis within each group revealed cream pigmentation as the most abundant (36%, 40%, and 27% for all the microorganisms, epiphytes, and endophytes, respectively). Beige and white-cream colonies were observed in 34% isolates (equally distributed between these two pigmentations) and only 5% of the colonies were white. The epiphytes were cream in 21%, white-cream in 12%, and white in 5%. The endophytes had white-cream pigmentation in 33% cases and were cream with no white colonies in 6.7%. The second “yellow” group was divided into yellow-cream, yellow, and yellow-orange sub-groups. Among them, pure yellow color was observed in 14% of all microbes – 7% of the epiphytes and 33% of the endophytes. The latter did not produce colonies in another hue of yellow. Bright yellow pigmentation was recorded for 7% of all isolates (9% of the epiphytes) whilst more orange colonies were found in 3.5% of the total number of the microorganisms (4.7% of the epiphytes).

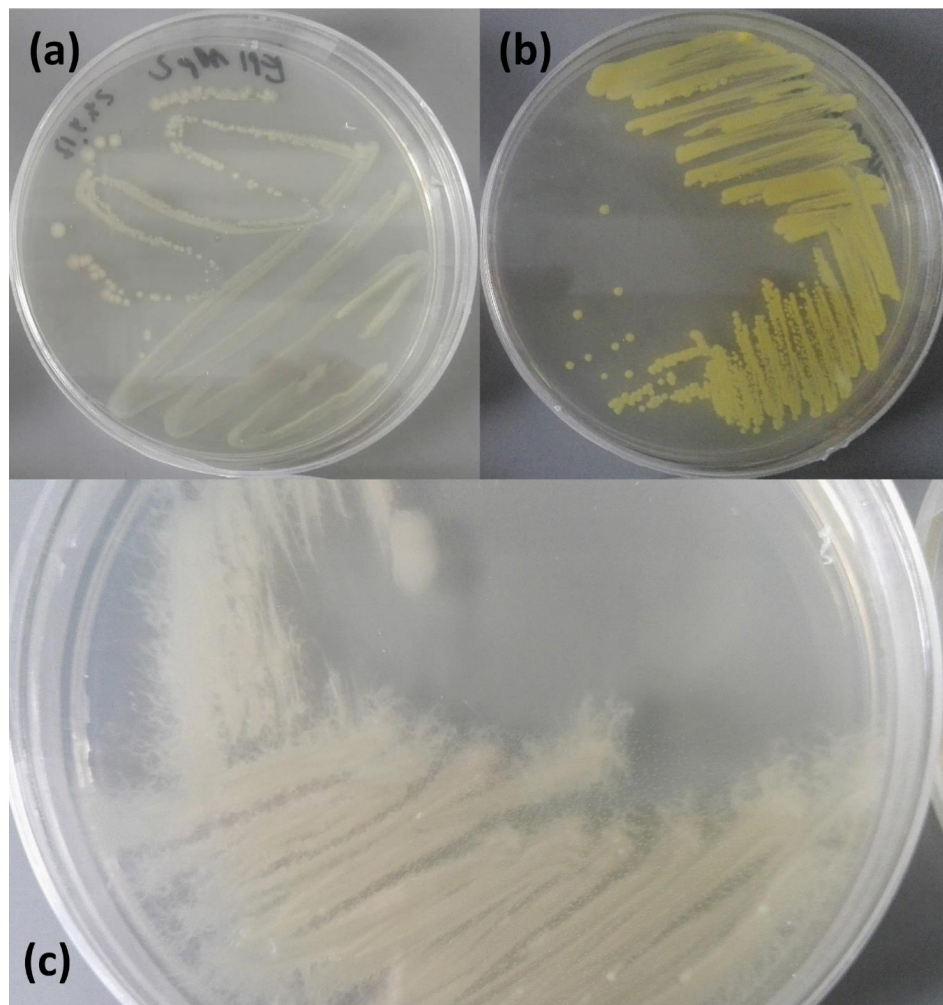


**Figure 3.** Examples of the most common isolates: (a) cream epiphyte, (b) yellow endophyte, and (c) white-cream filamentous form of epiphyte no. 37. Photo: A. Banach.

The next studied trait was colony elevation: Flat (F), raised (R), convex (C), and umbonate (U). We found raised colonies as the most abundant (52%). As much as 80% of the endophytes and 42% of the epiphytes were characterized by such colony elevation. Also, 26% of the isolates were flat, 17% were umbonate, and only 5% were convex. Flat, umbonate, and convex colonies were detected in 30%, 21%, and 7% of the epiphytes, respectively. No convex colonies were recorded in the endophytes; 13% were flat and 7% were umbonate.

The margin was the last morphological trait assessed. We observed colonies with entire, undulate, and filiform margins. The first margin type was found to be the most common (71%)—67% of the epiphytes and as much as 80% of the endophytes displayed this margin type. The undulate margin was noted in 30% of the counts (30% of the epiphytes and 20% of the endophytes). The filiform margin was observed only in one case, and this epiphyte formed a filamentous colony (2%) (Figure 3c).

For additional characterization, we determined the type of the cell wall using Gram staining. We found Gram-positive bacteria as the dominant group—66% of the counts (56% of the epiphytes and 93% of the endophytes).

### 2.3. Identification of Isolates

On the basis of 16S rRNA (hypervariable fragments V2-V4) analysis, we showed 99% similarity of the sequences (Table A1). Analysis of the 16S rDNA gene fragment revealed three identical epiphytic isolates number 22, 30, and 32; only no. 22 was entered into GenBank database. In addition, we did not obtain sufficiently good sequences for reliable characterization epiphytes no. 8, 15, 26, 27, 31, 33, 39, and 40 as well as one endophyte no. 15. As a result, 35 epiphytes and 14 endophytes (85% of isolated microorganisms) were successfully identified and entered to the database. Their names and the accession numbers are presented in Table 3.

**Table 3.** List of identified microorganisms (accession numbers from GenBank, NCBI). Column ‘No.’ represents the number of isolate corresponding to these in Table 2. Note some missing numbers due to unsuccessful identification.

No.	Isolate name	Accession no.	No.	Isolate name	Accession no.
Epiphytes			Epiphytes—continuation		
1	<i>Achromobacter</i> sp. AzoEpi1	MG881884	29	<i>Agrobacterium</i> sp. AzoEpi25	MG881908
2	<i>Bacillus</i> sp. AzoEpi2	MG881885	31	<i>Agrobacterium</i> sp. AzoEpi34	MH605442
3	<i>Bacillus</i> sp. AzoEpi3	MG881886	34	<i>Achromobacter</i> sp. AzoEpi26	MG881909
4	<i>Bacillus</i> sp. AzoEpi4	MG881887	35	<i>Bacillus</i> sp. AzoEpi27	MG881910
5	<i>Bacillus</i> sp. AzoEpi5	MG881888	36	<i>Bacillus</i> sp. AzoEpi28	MG881911
6	<i>Microbacterium</i> sp. AzoEpi6	MG881889	37	<i>Bacillus</i> sp. AzoEpi29	MG881912
7	<i>Delftia</i> sp. AzoEpi7	MG881890	38	<i>Bacillus</i> sp. AzoEpi30	MG881913
8	<i>Bacillus</i> sp. AzoEpi33	MH605441	41	<i>Bacillus</i> sp. AzoEpi35	MH605443
9	<i>Bacillus</i> sp. AzoEpi8	MG881891	42	<i>Bacillus</i> sp. AzoEpi31	MG881914
10	<i>Achromobacter</i> sp. AzoEpi9	MG881892	43	<i>Bacillus</i> sp. AzoEpi32	MG881915
11	<i>Bacillus</i> sp. AzoEpi10	MG881893	Endophytes		
12	<i>Achromobacter</i> sp. AzoEpi11	MG881894	1	<i>Bacillus</i> sp. AzoEndo1	MG859252
13	<i>Agrobacterium</i> sp. AzoEpi12	MG881895	2	<i>Staphylococcus</i> sp. AzoEndo10	MH605510
14	<i>Achromobacter</i> sp. AzoEpi13	MG881896	3	<i>Staphylococcus</i> sp. AzoEndo11	MH605511
16	<i>Bacillus</i> sp. AzoEpi14	MG881897	4	<i>Staphylococcus</i> sp. AzoEndo12	MH605512
17	<i>Bacillus</i> sp. AzoEpi15	MG881898	5	<i>Staphylococcus</i> sp. AzoEndo13	MH605513
18	<i>Bacillus</i> sp. AzoEpi16	MG881899	6	<i>Micrococcus</i> sp. AzoEndo9	MG881919
19	<i>Bacillus</i> sp. AzoEpi17	MG881900	7	<i>Micrococcus</i> sp. AzoEndo14	MH605514
20	<i>Agrobacterium</i> sp. AzoEpi18	MG881901	8	<i>Bacillus</i> sp. AzoEndo2	MG859253
21	<i>Bacillus</i> sp. AzoEpi19	MG881902	9	<i>Bacillus</i> sp. AzoEndo3	MG859254
22	<i>Bacillus</i> sp. AzoEpi20	MG881903	10	<i>Micrococcus</i> sp. AzoEndo7	MG881917
23	<i>Alcaligenes</i> sp. AzoEpi21	MG881904	11	<i>Bacillus</i> sp. AzoEndo4	MG859255
24	<i>Achromobacter</i> sp. AzoEpi22	MG881905	12	<i>Bacillus</i> sp. AzoEndo5	MG859256
25	<i>Microbacterium</i> sp. AzoEpi23	MG881906	13	<i>Bacillus</i> sp. AzoEndo6	MG859257
28	<i>Bacillus</i> sp. AzoEpi24	MG881907	14	<i>Acinetobacter</i> sp. AzoEndo8	MG881918

The identification procedure revealed that the isolates represented 9 genera (6 for epiphytes, 4 for endophytes; note that some epi- and endophytic microorganisms belong to the same genus). Based on their numbers, it can be concluded that the dominant epiphytic phylum was Firmicutes (60%) followed by Proteobacteria (34%) and Actinobacteria (6%). In the case of the endophytes, Firmicutes (86%) were dominant as well, whereas Proteobacteria and Actinobacteria constituted equally 7%. Within Firmicutes, *Bacillus* was the only representative genus in the case of the epiphytes (21 isolates). This phylum in the endophytes was equally represented by *Bacillus* (6 isolates, 43%) and *Staphylococcus* (4 isolates, 29%). The epiphytes belonging to Proteobacteria were classified into the order Rhizobiales (Alphaproteobacteria) represented by the genus *Agrobacterium*—11% (4 isolates) and Burkholderiales (Betaproteobacteria) represented by *Alcaligenes* (1), *Achromobacter* (6), and *Delftia* (1 isolate) (23%). *Acinetobacter* was the only genus representative for endophytic Proteobacteria (1 isolate), *Microbacterium* (2) represented epiphytic Actinobacteria, and *Micrococcus* (3 isolates) represented endophytes from this phylum.

#### 2.4. Synthesis of Plant Growth Promoters

In our study, we intended to present the potential of the isolated microorganisms in the synthesis of plant growth-promoting substances, which is very poorly recognized in the case of *A. filiculoides*. Consequently, the levels of IAA, cellulase and protease activities, utilization of P, and production of siderophores were determined. To this end, we selected one representative of each identified genera, i.e., 6 epiphytes and 4 endophytes.

The quantification of IAA synthesis revealed 3 promising strains: *Micrococcus* sp. AzoEndo14, *Delftia* sp. AzoEpi7, and *Agrobacterium* sp. AzoEpi25. The first one produced the highest amounts of auxin ( $17.9 \mu\text{g}\cdot\text{mL}^{-1}$ ); in turn, the other two yielded  $3.575$  and  $6.39 \mu\text{g}\cdot\text{mL}^{-1}$  of the compound, respectively (Table 4). To assess the capability of the microorganisms of lysis of the pathogen cell wall, we assayed cellulase and protease activities. Importantly, a positive reaction was recorded in all the isolates studied (Table 4).

**Table 4.** Levels of IAA as well as cellulase and protease activities of the isolates studied (means  $\pm$  SD).

Isolate (Genera)	IAA ( $\mu\text{g mL}^{-1}$ )	Cellulase Activity		Protease Activity	
		h <sup>1</sup> (cm)	h:c <sup>2</sup>	h (cm)	h:c
<i>Staphylococcus</i> sp. AzoEndo11	n/a <sup>3</sup>	0.98 (0.25)	1.19 (0.33)	1.25 (0.21)	0.45 (0.23)
<i>Micrococcus</i> sp. AzoEndo14	17.900 (0.201)	1.50 (0.14)	1.05 (0.25)	1.00 (0.19)	0.31 (0.08)
<i>Bacillus</i> sp. AzoEndo3	n/a	1.06 (0.20)	1.06 (0.05)	1.76 (0.36)	1.01 (0.89)
<i>Acinetobacter</i> sp. AzoEndo8	n/a	1.20 (0.00)	0.80 (0.00)	1.32 (0.34)	0.58 (0.19)
<i>Achromobacter</i> sp. AzoEpi1	n/a	1.03 (0.13)	0.67 (0.08)	1.22 (0.19)	0.40 (0.09)
<i>Bacillus</i> sp. AzoEpi2	n/a	0.80 (0.08)	0.47 (0.07)	1.10 (0.19)	0.28 (0.15)
<i>Delftia</i> sp. AzoEpi7	3.575 (0.029)	0.23 (0.13)	0.27 (0.17)	1.12 (0.26)	0.41 (0.18)
<i>Alcaligenes</i> sp. AzoEpi21	n/a	0.65 (0.06)	1.20 (0.23)	1.57 (0.31)	0.45 (0.18)
<i>Microbacterium</i> sp. AzoEpi23	n/a	0.50 (0.08)	1.20 (0.29)	1.33 (0.34)	0.78 (0.35)
<i>Agrobacterium</i> sp. AzoEpi25	6.390 (0.053)	0.68 (0.15)	1.33 (0.47)	2.95 (0.28)	1.10 (0.33)

<sup>1</sup> h—halo size; <sup>2</sup> h:c—halo-to-colony size ratio; <sup>3</sup> n/a—no positive reaction.

The diameter of the halo after cellulose decomposition ranged from 0.23–1.5 cm. The endophytes were characterized by stronger cellulase activity; we observed zones from 0.98 (*Staphylococcus* sp. AzoEndo11) to 1.5 cm (*Micrococcus* sp. AzoEndo14). It was demonstrated that the halo was lower by 20% only for *Acinetobacter* sp. AzoEndo8 in comparison to the colony diameter. The zone in the other 3 isolates was by 5–19% higher than the size of developed colonies. In the case of the epiphytes, the lowest activity was noted for *Delftia* sp. AzoEpi7 (0.23 cm) and the highest value of 1.03 cm was found for *Achromobacter* sp. AzoEpi1. We noticed that *Achromobacter* sp. AzoEpi1, *Bacillus* sp. AzoEpi2, and *Delftia* AzoEpi7 developed smaller halos in relation to their colonies, i.e., with the h:c ratios of 0.67, 0.47, and 0.27, respectively. The other three, i.e., *Alcaligenes* sp. AzoEpi21, *Microbacterium* sp. AzoEpi23,

and *Agrobacterium* sp. AzoEpi25, formed halos that were larger by 20–33% (Table 4). Protein substrate consumption was indicated by halos larger than 1 cm in all samples. The endophytic *Micrococcus* sp. AzoEndo14 generated the smallest zone (1 cm), which was 69% smaller than that of the colonies. *Bacillus* sp. AzoEndo3, in contrast, developed the biggest zone of 1.76 cm (1% bigger than that of the colonies). However, the epiphytic *Bacillus* sp. AzoEpi2 showed the lowest protease activity with a 1.1 cm halo (72% smaller zone than that of the colonies). *Agrobacterium* sp. AzoEpi25 produced the biggest zones 2.95 cm with the highest h:c ratio of 1.1 (Table 4).

Importantly, all the isolates demonstrated potential for organic P mineralization; the endophytes had halos ranging from 0.26 cm (*Staphylococcus* sp. AzoEndo11) with a h:c ratio of 0.23–0.62 cm (*Bacillus* sp. AzoEndo3) and an h:c ratio of 0.47. The epiphytes mineralized more phosphate on average: The halos ranged from 0.35 (*Alcaligenes* sp. AzoEpi21) to 0.52 cm (*Bacillus* sp. AzoEpi2) with h:c ratios of 0.33–0.43, respectively. Inorganic P appeared to be more difficult to solubilize; the endophytic *Acinetobacter* sp. AzoEndo8 was unable to utilize it and only the epiphytic *Delftia* sp. AzoEpi7 was able to develop a halo of 0.79 cm, which was by 10% larger than that of its colonies. The rate of P solubilization by the endophytes ranged between 0.29 cm (*Micrococcus* sp. AzoEndo14), i.e., 64% of the colony sizes and 1.95 cm (*Staphylococcus* sp. AzoEndo11), i.e., 91% larger than in the colonies (Table 5). This study allowed us to qualify all isolates as PMB, and only *Staphylococcus* sp. AzoEndo11, *Micrococcus* sp. AzoEndo14, and *Bacillus* sp. AzoEndo3 (endophytes) were qualified as PSM, whereas *Delftia* sp. AzoEpi7 was the only PMPSB.

**Table 5.** Levels of IAA as well as cellulase and protease activities of studied isolates (means±SD).

Isolate	P mineralization		P solubilization		Siderophores	
	h <sup>1</sup> (cm)	h:c <sup>2</sup>	h (cm)	h:c	h (cm)	h:c
<i>Staphylococcus</i> sp. AzoEndo11	0.26 (0.19)	0.23 (0.17)	1.95 (0.72)	1.91 (0.93)	n/a <sup>3</sup>	n/a
<i>Micrococcus</i> sp. AzoEndo14	0.39 (0.08)	0.32 (0.12)	0.29 (0.44)	0.64 (0.62)	n/a	n/a
<i>Bacillus</i> sp. AzoEndo3	0.62 (0.18)	0.47 (0.18)	1.15 (0.54)	1.35 (0.43)	3.56 (0.17)	10.10 (1.79)
<i>Acinetobacter</i> sp. AzoEndo8	0.31 (0.10)	0.25 (0.09)	n/a	n/a	n/a	n/a
<i>Achromobacter</i> sp. AzoEpi1	0.36 (0.09)	0.33 (0.11)	n/a	n/a	0.56 (0.29)	0.07 (0.04)
<i>Bacillus</i> sp. AzoEpi2	0.52 (0.18)	0.43 (0.15)	n/a	n/a	n/a	n/a
<i>Delftia</i> sp. AzoEpi7	0.49 (0.19)	0.43 (0.16)	0.79 (0.29)	1.01 (0.39)	0.98 (0.21)	0.64 (0.10)
<i>Alcaligenes</i> sp. AzoEpi21	0.35 (0.13)	0.31 (0.13)	n/a	n/a	0.10 (0.00)	0.39 (0.15)
<i>Microbacterium</i> sp. AzoEpi23	0.46 (0.13)	0.43 (0.15)	n/a	n/a	n/a	n/a
<i>Agrobacterium</i> sp. AzoEpi25	0.43 (0.13)	0.39 (0.15)	n/a	n/a	0.41 (0.14)	0.17 (0.06)

<sup>1</sup> h—halo size; <sup>2</sup> h:c—halo-to-colony size ratio; <sup>3</sup> n/a—no positive reaction.

Production of siderophores was visualized only in some samples: One endophyte, i.e., *Bacillus* sp. AzoEndo3 (a huge halo of 3.56 cm with low colony growth—10 times lower colony size), and 3 epiphytes produced the compounds. Among them, *Delftia* sp. AzoEpi7 produced the largest halo (0.98 cm), which represented 64% of the colony size. *Achromobacter* sp. AzoEpi1 followed by *Alcaligenes* sp. AzoEpi21 produced large halos as well (0.1 and 0.56 cm, respectively).

### 3. Discussion

One of our goals was to identify the cyanobiont co-existing with *A. filicoides*. Given the contrasting information from the literature, this issue is still not completely clear. In the study by Pereira and Vasconcelos [16], deep screening of the classification and phylogeny of the cyanobiont was carried out. The existing controversy over its classification is associated with the method applied. In addition, co-evolution between the cyanobiont and the *Azolla* host is possible as well as the existence of more than one genus or more than one species strain. This could explain the different classifications originating from molecular and botanical analysis. Although many publications traditionally name this cyanobacteria *Anabaena azollae* or *Nostoc azollae* [10], likewise new publications [26], Komárek and

Anagnostidis [27] renamed it to *Trichormus azollae*. The results reported by Baker and colleagues [15] are consistent with the latter study. In addition, most of non-planktonic species of *Anabeana* without gas vacuoles are now included in *Trichormus*. All planktonic species with gas vacuoles retain their classification into *Anabeana*. The difference between the two genera, *Trichormus* and *Anabeana*, as presently understood, is related to the developmental relationships between the heterocysts and spores [28]. The botanical observation carried out in this study revealed these traits, allowing a conclusion that *T. azollae* is the cyanobiont. It is also convincing that the AlgaeBase states that *A. azollae* is currently regarded as a synonym of *T. azollae* [29].

The main goal in our study was to detect and identify cultured microbiome of *A. filiculoides*. Previous studies mentioned the presence of bacterial endosymbionts within fern's cavities; yet, they have not been identified. This could be attributed to insufficient identification tools available at that time, whereas many modern tools are available now. Studies conducted by Serrano et al. and Carrapiço [19,20] typed some bacterial genera: *Pseudomonas*, *Alcaligenes*, *Caulobacter*, and *Arthrobacter*. Nierzwicki-Bauer and Aulfinger [18] presented a description of 5 different microorganisms, i.e., both G+ and G- bacteria inhabiting leaf cavities of *A. caroliniana*. All these studies were based on the use of biochemical and microbiological tests for describing these microorganisms. Nevertheless, none of them employed any molecular analysis for identification of bacteria. However, an interesting paper has recently been published by Dijkhuizen and colleagues [26], who performed a metagenomic study of the *A. filiculoides* genome. They found Burkholderiales, Caulobacteriales, and Rhizobiales as the most abundant microbial groups accompanying the fern. Deeper analysis revealed microorganisms belonging to the genera *Microbacterium*, *Hypomicrobium*, *Shinella*, *Ralstonia*, *Rhizobium*, and *Hydrocarboniphaga* [26]. We found these data different from ours. In our study, Burkholderiales constituted 23% and Rhizobiales 11% of the epiphytic microbiome, which is one-third of the whole microbiome identified. In addition, we obtained two isolates belonging to *Microbacterium*. Moreover, other genera, including *Delftia* were not detected. The differences in microbiome composition may be connected with *Azolla* sp. environment. Our laboratory culture was sustained for 9 years on IIRI medium. Dijkhuizen and colleagues [26] tested bacterial communities with both natural (ditch) and controlled (sterilized, IIRI collections). They stated that *Azolla* sp. has control over the bacterial community assembly within its closed leaf pockets and it differs between sources of *Azolla* sp. Since there are no more similar studies, we consider our study as a next very important step providing deep knowledge on the *A. filiculoides* microbiome.

For microbiome phenotyping, we found only one paper describing the capability of *A. filiculoides* and *A. pinnata* endosymbiotic *Arthrobacter* sp. for IAA production, where the auxin concentration remained at the level of 1.5–10  $\mu\text{g mL}^{-1}$  at an L-tryptophan dose of 100–600  $\mu\text{g}\cdot\text{mL}^{-1}$  [30]. Other studies demonstrated different efficiencies of IAA production by various microorganisms. In the study by Ghodsalavi et al. [31], the highest production of IAA (>20  $\mu\text{g mL}^{-1}$ ) was recorded for *Pseudomonas* sp., whereas these values in *Bacillus* sp. and *Agrobacterium* sp. amounted to 3–7 and 16  $\mu\text{g mL}^{-1}$ , respectively. Dutta et al. [32] showed IAA production of 87.9  $\mu\text{g mL}^{-1}$  for *Bacillus* sp. In turn, Morel et al. [33] proved that *Delftia* sp. JD2 was able to synthesize IAA up to 80  $\mu\text{g}\cdot\text{mg}^{-1}$  dw when exposed to Cr(VI) ions. Strains from the genus *Bacillus* were reported to display both cellulase and protease activity [32,34]. Ghodsalavi et al. [31] reported high protease activity in *Bacillus* sp., which produced 2–3 cm diameter halos, i.e., approximately twice as big as in our study. *Agrobacterium* sp. formed 2.3 cm halos, whilst 2.95 cm zones were noted in our study. In contrast to our study, Cho et al. [34] indicated no ability to decompose the pathogen cell wall by *Microbacterium* sp. The ability to solubilize P in *Bacillus* sp. was reported by Dutta et al. [32]. PSB, PSM, and PMPSB microorganisms were reported in the study of Jorquera and colleagues [35]; however, the authors mentioned only strains from the genera *Pseudomonas*, *Enterobacter*, and *Pantoea*, whereas Chen et al. [36] presented *Delftia* sp. as PSB for the first time. The production of siderophores by *Bacillus* sp. was reported by Ghodsalavi et al. [31] and Dutta et al. [32]. Morel et al. [33] reported that *Delftia* sp. JD2 produced siderophores in Cr(VI) stress conditions.

It is worth emphasizing that other authors presented the ability to promote plant growth by microorganisms originating from soil or isolated from terrestrial vegetation. However, the data regarding aquatic microorganisms are scarce. Most of the microorganisms described were not found in the *A. filiculoides* microbiome and only *Bacillus* sp. was often identified.

By displaying the highest potential in growth promotion among all isolates, *Delftia* sp. AzoEpi7 particularly attracted our attention. Members of the genus *Delftia* are aerobic non-endospore forming Gram-negative rods that inhabit diverse ecological niches. Taxonomically, this genus belongs to the Comamonadaceae family within the Burkholderiales order of the Betaproteobacteria class. Currently, it comprises five species: *D. acidovorans*, *D. tsuruhatensis*, *D. lacustris*, *D. litopenaei*, and *D. deserti* [37]. *Delftia* sp. is known as a halotolerant bacterium with the capability of organic biodegradation [38]. It has also been reported that *Delftia* sp. have potential roles in bioremediation of organic and inorganic pollutants and production of industrially valuable compounds [39]. In addition, the *Delftia* sp. genome sequencing (6–6.7 Mb, GC content of approximately 66%) proved that particular genetic elements are involved in diverse biodegradation pathways and resistance to heavy metals [37,40], production of phytohormones and siderophores [33], and production of antimicrobial compounds [41]. In 2013, Johnston et al. [42] reported that *D. acidovorans* exhibited resistance against gold by producing a secondary metabolite allowing biomineralization of the metal from liquid. Recently, Li and colleagues [43] have proved that *D. tsuruhatensis* GX-3 is able to bioaccumulate gold forming nanoparticles outside its cell. This makes *Delftia* sp. extremely interesting bacteria from the biotechnological and engineering point of view, since all ways for reclaiming precious metals are tempting and wanted. Another interesting potential of *Delftia* sp. was demonstrated in the study conducted by Jangir and colleagues [44]. It appeared to use an extracellular electron transfer (EET) strategy for energy harvesting via generation of anodic current using acetate as an electron donor. This may indicate the potential of *Delftia* sp. in electricity generation via Microbial Fuel Cells (MFC). All this information proves the high importance of these bacteria. Another feature of *Delftia* sp. is the production of nanopods, i.e., extracellular structures important in cell-to-cell interactions, when grown on phenanthrene [45].

Since there are studies on microbially-assisted phytoremediation, it would be worth studying the role of the microbiome in metal remediation [7,9,46], which what would be beneficial for designing better metal-removing biological systems. Moreover, our previous studies [11] showed high potential of *Azolla* sp. in the reduction of metal levels in waters, which encourages us to study the newly discovered microbiome and *Delftia* sp. AzoEpi7 in detail.

## 4. Materials and Methods

### 4.1. Plant Material

*A. filiculoides* originated from our laboratory culture established in 2010 using material obtained from Warsaw Botanical Garden (Poland). Plants were grown according to the recommendation of the International Rice Research Institute [47] (Appendix A). After 3 weeks, the biomass obtained was used for microbial isolation.

All reagents were dedicated for microbiological analyses and purchased from Sigma-Aldrich; water was deionized and sterilized before use (sdH<sub>2</sub>O).

### 4.2. *Azolla* Cyanobiont

The isolation of the cyanobiont was performed by crushing the plant material (sterilized three times in 0.12% NaClO, 0.01% Triton X-100 for 10 min, next in 70% ethanol and sdH<sub>2</sub>O) between two sterile microscopic slides and washing with nitrogen-free BG11<sub>0</sub> medium [47]. Next, the material was incubated in batch culture using 15 mL BG11<sub>0</sub> medium (1:6, culture: Medium ratio) at 23 °C and 63 μmol quantum photosynthetically active radiation (PAR) per m<sup>2</sup> s at a 24/0h photoperiod (n = 5). After 7 days, the cells were passaged by inoculating 20 mL of fresh BG11<sub>0</sub> medium with 2.5 mL

inoculum ( $n = 4$ ). One week later, the next subculture was performed (6.5 mL of inoculum + 40 mL of both media, 7 days). Importantly, after each step, the samples were taken for microscopic observations and after the last passage, the material was used for isolation of cyanobacterial DNA.

#### 4.3. Isolation of Microorganisms

Prior to the isolation of the endophytic microorganisms, the plant material was sterilized in a laminar chamber. For this operation, 3 healthy plants were randomly chosen from the culture in order to provide repeatability. The material was washed in  $\text{sdH}_2\text{O}$  and separated into shoots and roots. Next, the plants' parts were immersed for a given time in subsequent reagents: (1) 0.1% Tween 80 for 30 s, (2) 1% NaClO for 5 min, (3) 70% ethanol—5 min, and (4)  $\text{sdH}_2\text{O}$ —5 min. The efficiency of sterilization was assessed by inoculating Petri dishes with the water from the last washing. Each sterilized plant part was ground in a mortar using 1 mL of phosphate buffer (pH 6.7). Next, three 250- $\mu\text{L}$  samples of each portion of the ground material were transferred into Eppendorf tubes.

The microorganisms present on the surface of *A. filiculoides* were isolated in two ways. The first method involved placing a few randomly chosen plants into a beaker with 10 mL of phosphate buffer; next, the plants were discarded after careful stirring. The second variant of isolation consisted of placing randomly picked plants onto the agar ( $n = 3$ ) setting their top part on the agar (see agar composition below).

#### 4.4. Cultivation and Description of Isolated Microorganisms

All material obtained from isolation described below were subjected to series dilutions up to  $10^{-4}$ . These diluted cultures (250  $\mu\text{L}$ ) were spread on sterile nutrient agar (25 mL per Petri dish) consisting of: Yeast extract (0.2%), beef extract (0.2%), peptone (0.5%), NaCl (0.4%) and agar (1.5%), pH 7.4 (BTL, Poland), supplemented with nystatin (50  $\text{mg}\cdot\text{mL}^{-1}$ ) to avoid fungal growth (as fungi were not the subject of this study) and incubated in the dark at 30 °C for 7 days (Hereus B20, Thermo Fisher Scientific, USA). Then, microbial colonies were inoculated into fresh medium and cultivated as above. The procedure was repeated until pure cultures were obtained.

The morphology of the colonies was described in terms of their shape (surface, elevation, margin, texture, size), pigmentation, and opacity. Their counts were made and referred to the total number of isolates (58) and total counts of both epi- (43) and endophytes (15). These numbers were further discussed as percentages, but they are presented in the table as individual counts. In order to describe the shape of the isolated cells and the type of their cellular wall, the Gram staining method was applied. The resulting slides were examined under a Nikon Eclipse 80i microscope equipped with UV2A, B2A, G2A, FITC and TRITC filters and photographs were taken using a digital camera with NIS-Elements software (Nikon Instruments Europe B.V., Amsterdam, The Netherlands). Cells with purple color were considered as Gram-positive, whilst red color indicated Gram-negative microorganisms.

The isolates were cultured on a liquid nutrient broth (0.2 % yeast extract, 0.2% beef extract, 0.5% peptone, 0.4% NaCl and 1.0% glucose, BTL, Poland) for 7 days at 30 °C (New Brunswick™ Innova® 42R, Eppendorf AG, Germany). During incubation, optical density ( $\text{OD}_{600}$ ) was determined spectrophotometrically (Shimadzu UV-1800, Japan) to construct growth curves for the microorganisms (Figure A1). For long-term storage, 700  $\mu\text{L}$  of each inoculum was mixed with 300  $\mu\text{L}$  of glycerol (3 replicates for the endophytes and 2 replicates for the epiphytes) and frozen at  $-80^\circ\text{C}$  (ZLN-UT 300, Pol-Eko-Aparatura, Poland). The other samples were used for subsequent analyses.

#### 4.5. Identification of the Cyanobiont

Only living material from the cultures was applied for taxonomic identification. Microscopic observations in a light field and using a UV lamp and UV2A filter were carried out using an Eclipse 80i Nikon microscope working with the magnification range up to 100x (Nikon Instruments Europe B.V., Amsterdam, The Netherlands). The microscope was connected to a digital microscope camera with

NIS-Elements software, used to observe and measure colonies, cells, and heterocyst of the studied cyanobacteria. The taxonomic designation was based on Komárek [48] and Hindak [49].

#### 4.6. Molecular Techniques

Total genomic DNA was isolated according to Stepniewska et al. [50] (Appendix A) followed by PCR reaction. The PCR mixture contained 1X Phusion Flash High-Fidelity PCR Master Mix (Thermo Scientific, USA), 1 µL of template DNA (1100 µg/mL on the average, Table A1), and sterile double-distilled water (free DNase) in a total volume of 25 µL. Universal eubacterial primers (each 1.0 µM): 27F and 518R (Table A2) were used. The reaction was carried out under the following conditions: 98 °C for 10 s; 30 cycles of 95 °C for 5 s, 56 °C for 5 s, and 72 °C for 40 s (LABCYCLER, SensoQuest GmbH, Germany). For amplification of cyanobiont DNA, the following four primers were used: Cyanobacterium-specific 23S30R and CYA359F, whilst *nif*-Df and *nif*-Dr were used for targeting the *nif* gene (Table A2). The PCR reactions were carried out as follows: 98 °C for 10 min; 30 cycles of 98 °C for 5 s, 55 °C for 5 s, and 72 °C for 60 s (*nif* primers) and 98 °C for 5 min; 30 cycles of 98 °C for 35 s, 54 °C for 45 s, and 72 °C for 60 s (16S rRNA primers). The PCR products were run on agarose gel (1%) and visualized with the use of SimplySafe™ (EURx, Poland). Additionally, control reactions were performed: Negative—containing only sterile double-distilled water (free DNase) without a DNA template and positive, in which DNA isolated from *E. coli* DH5α™ was a template. Then, all PCR products were purified and sent to sequencing (Genomed S.A., Poland). The sequences were analyzed by the web-version of BLASTN algorithm (NCBI, USA) for identification of the isolates. The identified sequences were deposited in the GenBank (NCBI, <http://www.ncbi.nlm.nih.gov/>) under the following accession numbers: MG859252-7, MG881884-915, MG881917-9, MH605441-3, and MH605510-14.

#### 4.7. Phenotypic Characterization

Bacterial strains in an exponential phase were applied for testing the ability of the microbiome to synthesize plant growth promoters. The production of indole-3-acetic acid (IAA) was initiated by inoculating liquid nutrient broth supplemented with 1 g l<sup>-1</sup> of L-tryptophan. Quantification of IAA was performed using Salkowski's reagent (35% HClO<sub>4</sub> + 0.5 M FeCl<sub>3</sub>·6H<sub>2</sub>O) and colorimetric analysis at 530 nm in reference to the calibration curve. Samples with pink color were considered positive for production of IAA [51] (Appendix A). Results were presented as means ± SD (standard deviation).

The ability to synthesize cellulolytic enzymes was assayed by growing the microorganisms (30 °C for 24 h) on nutrient agar supplemented with 1% carboxymethylcellulose (CMC) sodium salt (cellulase activity indicator medium). Lugol's solution was applied for visualization of cellulose activity. A positive reaction was observed when the colonies of the isolates were surrounded by a yellow halo against a dark background [52]. Protease activity was determined by culturing selected isolates on nutrient agar supplemented with 5% skim milk at 30 °C in darkness (protease activity indicator medium). The development of clear zones around the colonies revealed protease activity.

Phosphate utilization by the microorganisms was determined using two P sources: Organic, sodium phytate, C<sub>6</sub>H<sub>18</sub>P<sub>6</sub>O<sub>24</sub>·12Na·xH<sub>2</sub>O (PSM medium) and inorganic calcium phosphate (Ca<sub>3</sub>(PO<sub>4</sub>)<sub>2</sub>) (NBRIP medium). The first was used for identification of P-mineralizing bacteria (PMB) and the second for P-solubilizing bacteria (PSB) [35]. The inoculated media were incubated at 30 °C for 4 days. The presence of clear zones around the colonies was taken as an indicator of phytate mineralization and phosphate solubilization. Based on these observations, we divided the microorganisms into PMB, PSM, and those using both P-sources (phosphate mineralizing, phosphate solubilizing bacteria, PMPSB).

Siderophore production was quantified using a CAS-agar assay of Alexander and Zuberer [53] (Appendix A). Positive results were indicated by formation of a clear halo around the colonies, showing a visual change in the color from dark blue to yellow.

For all plate tests, Petri dishes were inoculated with 15 µL of the cell suspension in 4 points. To quantify the enzymatic activities, the sizes of colonies and halos were assessed and halo-to-colony size ratios (n = 3) were calculated. The data are presented as means ± SD.

## 5. Conclusions

Our experiment has proved that *A. fliucloides* is inhabited by not only its cyanobiont but also by bacteria present both on its surface (epiphytes) and inside the plant (endophytes).

In general, the isolates represented Gram-positive bacteria mostly with a punctiform size (epiphytes, also small size) with a circular shape, raised with a glistering and smooth surface (epiphytes, also rough) with butyrous texture, opaque, and cream pigmentation (endophytes, also yellow and white-cream) with an entire margin.

The similarity analysis allowed us to classify the isolates into 9 bacterial genera. The epiphytes belonged to *Achromobacter*, *Bacillus*, *Microbacterium*, *Delftia*, *Agrobacterium*, and *Alcaligenes*, while the endophytes were classified as *Bacillus*, *Staphylococcus*, *Micrococcus*, and *Acinetobacter*.

The tests applied for the determination of plant growth promotion features revealed high importance and benefits of the tested microbiome for plants. All isolates were able to synthesize enzymes responsible for cell wall lysis (cellulase and protease). In addition, all of them showed P mineralization potential and some exhibited P solubilization capability. Three bacterial strains (*Micrococcus* sp. AzoEndo14, *Delftia* sp. AzoEpi7, *Agrobacterium* sp. AzoEpi25) synthesized IAA. Siderophores were only produced by endophytic *Bacillus* sp. AzoEndo3 and epiphytic *Achromobacter* sp. AzoEpi1, *Delftia* sp. AzoEpi7, *Alcaligenes* sp. AzoEpi21, and *Agrobacterium* sp. AzoEpi25. *Delftia* sp. AzoEpi7 seemed to be the only strain with the ability to synthesize all studied growth promoters; hence, we recommend it as the most beneficial for host plants.

**Author Contributions:** The concept of the study was made by A.B. and A.K., the methodology was selected and applied by A.B. and A.K. (isolation of microorganisms, cultivation, description, molecular studies, phenotyping); the cyanobiont was identified by R.M. The results were analyzed and described by A.B., A.K., R.M. and A.W. The manuscript was written by A.B. and reviewed by A.K., A.W. and R.M.

**Funding:** This research received no external funding.

**Conflicts of Interest:** The authors declare no conflict of interest.

## Abbreviations

IAA	indole-3-acetic acid
P	phosphorus
PGPB	Plant Growth-Promoting Bacteria
BUT	Butyrous
MUC	Mucoid
BRIT	Brittle
OPQ	opaque
TRANS	translucent
IRID	iridescent
F	flat
R	raised
C	convex
U	umbonate
sdH <sub>2</sub> O	deionized and sterilized water
OD	optical density
SD	standard deviation
CMC	carboxymethylcellulose
PMB	P-mineralizing bacteria
PSM	P-solubilizing bacteria
PMPSB	phosphate mineralizing, phosphate solubilizing bacteria

## Appendix A

### Cultivation of *A. filiuloides*

Plants were grown in glass aquaria (20 × 30 × 15 cm) on recommended IRRI medium [47] without nitrogen supply supplemented in 0.1 mL l<sup>-1</sup> anti-algal agent, Algin (Topical®, Poland), containing CuSO<sub>4</sub>·5H<sub>2</sub>O as the active substance. Fluorescent Philips lamps Master TL-D 36W/830 were used to provide 3500 lux light energy (corresponding to 14 W m<sup>-2</sup> or 6.3 μmol quantum of photosynthetically active radiation, PAR per m<sup>2</sup> s) at 16/8 h photoperiod, temperature of 20.69 ± 1.55 °C, and relative humidity of 84.5 ± 5.16% (H-881t hygrometer, Zootechnika, Poland).

### Isolation of Bacterial DNA

The method is based on an original method proposed by Sambrook et al. [54]. Cells from 10 mL samples of late exponential cultures were collected by centrifugation. The pellet was suspended in 250 μL of TE buffer containing 50 mM Tris-HCl (pH = 8.0) and 50 mM EDTA (pH = 8.0). To achieve complete lysis of the cells, 1 mL of GES buffer (pH = 8.0) containing 5 M guanidine thiocyanate, 100 mM EDTA, and 0.5% sarkosyl was added. The mixture was incubated at room temperature for 10 minutes and then “crude lysates” were cooled on ice. After addition of 125 μL of ammonium acetate (7.5 M), the samples were mixed and further incubated on ice. The DNA obtained was purified with 250 μL of a chloroform-isoamyl alcohol (24:1) mixture, precipitated with isopropanol, washed with cold ethanol, and dissolved in 50 μL of sterile distilled water.

### Phenotypic Analysis

**IAA production.** The cultures (n = 3) were incubated at 30 °C for 5 days in darkness on a rotary shaker (125 rpm) on liquid nutrient broth supplemented with 1 g·L<sup>-1</sup> of L-tryptophan. Next, the samples were centrifuged at 10,000 rpm for 10 minutes and 2 mL of the supernatant were mixed with 4 mL of Salkowski’s reagent (50 mL 35% HClO<sub>4</sub>, 1 mL 0.5 M FeCl<sub>3</sub>·6H<sub>2</sub>O) [55]. After leaving the mixture at 30 °C for 30 minutes in darkness, the concentration of IAA was measured colorimetrically at 530 nm (Shimadzu UV/VIS-1800, Japan) using a calibration curve ranging up to 100 μg·mL<sup>-1</sup>. The calibration was prepared by processing the IAA solution in the same manner as the samples.

**Siderophore production.** 4 solutions were made: Fe-CAS indicator (1.21 mg·mL<sup>-1</sup> of CAS in 1 mM FeCl<sub>3</sub>·6H<sub>2</sub>O in 10 mM HCl), HDTMA (1.82 mg·mL<sup>-1</sup>), buffer (30.24 g of PIPES, 0.3 g KH<sub>2</sub>PO<sub>4</sub>, 0.5 g NaCl, and 1.0 g NH<sub>4</sub>Cl, pH 6.8), medium (493 mg MgSO<sub>4</sub>·7H<sub>2</sub>O, 11 mg CaCl<sub>2</sub>, 1.17 mg MnSO<sub>4</sub>·H<sub>2</sub>O, 1.4 mg H<sub>3</sub>BO<sub>3</sub>, 0.04 mg CuSO<sub>4</sub>·5H<sub>2</sub>O, 1.2 mg ZnSO<sub>4</sub>·7H<sub>2</sub>O, and 1.0 mg Na<sub>2</sub>MoO<sub>4</sub>·2H<sub>2</sub>O) and 10% (w:v) casamino acids. All solutions were autoclaved separately, cooled to 50 °C, and mixed together.

## Appendix B

**Table A1.** Similarity of the obtained isolates to the sequences deposited in GenBank (NCBI) and the concentration of obtained DNA.

Code <sup>1</sup>	Similar to	Similarity	Accession	c DNA (μg/mL)
EP1	<i>Achromobacter</i> sp. IR27	97%	GU726513.1	55
EP2	<i>Bacillus cereus</i> strain F2-2-21	99%	KX350029.1	1465
EP3	<i>Bacillus simplex</i> strain Se2	99%	HQ432812.1	380
EP4	<i>Bacillus subtilis</i> strain SUT2	99%	GU971415.1	940
EP5	<i>Bacillus subtilis</i> strain RW134	99%	MH010185.1	50
EP6	<i>Microbacterium oxydans</i> strain CanS-105	99%	KT580637.1	3640
EP7	<i>Delftia acidovorans</i> isolate RI41	99%	DQ530127.1	20
EP8	<i>Bacillus thuringiensis</i> strain WY9	100%	JQ936681.1	2288
EP9	<i>Bacillus subtilis</i> strain BGR261	99%	KT074466.1896	25
EP10	<i>Achromobacter</i> sp. strain SYP-B562	99%	KY636382.1	1560
EP11	<i>Bacillus subtilis</i> strain RW134	99%	MH010185.1	170
EP12	<i>Achromobacter</i> sp. strain SYP-B562	98%	KY636382.1	35
EP13	<i>Agrobacterium tumefaciens</i> strain BF-R21	100%	KY292437.1	3280
EP14	<i>Achromobacter spanius</i> strain 2S9	96%	KM374759.1	980
EP15	n/a <sup>2</sup>	n/a	n/a	655
EP16	<i>Bacillus</i> sp. R-45540	100%	FR774944.1	260
EP17	<i>Bacillus subtilis</i> strain RW134	99%	MH010185.1	120
EP18	<i>Bacillus pumilus</i> strain IHBB 11092	99%	KR085935.1	3325
EP19	<i>Bacillus thuringiensis</i> strain F9	99%	HQ432809.1	285
EP20	<i>Agrobacterium tumefaciens</i> strain BF-R21	100%	KY292437.1	820

Table A1. Cont.

Code <sup>1</sup>	Similar to	Similarity	Accession	c DNA (µg/mL)
EP21	<i>Bacillus cereus</i> strain AM11	99%	JQ435688.1	5965
EP22	<i>Bacillus cereus</i> strain F1-1-1	99%	KX349989.1	340
EP23	<i>Alcaligenes</i> sp. DH1f	99%	KF557586.1	510
EP24	<i>Achromobacter</i> sp. strain SYP-B562	100%	KY636382.1	560
EP25	<i>Microbacterium oxydans</i> strain AE038-20	100%	KX369591.1	160
EP26	<i>Achromobacter</i> sp. ATY31	98%	HQ219950.1	1698
EP27	n/a	n/a	n/a	80
EP28	<i>Bacillus cibi</i> strain AIMST Ngme2	98%	JF939005.1	30
EP29	<i>Agrobacterium tumefaciens</i> strain BF-R21	100%	KY292437.1	1590
EP30	<i>Achromobacter</i> sp. strain SYP-B562	98%	KY636382.1	100
EP31	<i>Agrobacterium tumefaciens</i> strain BF-R21	100%	KY292437.1	358
EP32	<i>Achromobacter</i> sp. strain SYP-B562	99%	KY636382.1	2510
EP33	n/a	n/a	n/a	70
EP34	<i>Achromobacter marplatensis</i> strain EY-T10	99%	KR476417.1	240
EP35	<i>Bacillus subtilis</i> strain BGR261	99%	KT074466.1	120
EP36	<i>Bacillus</i> sp. strain APNK5	94%	MG193758.1	340
EP37	<i>Bacillus weihenstephanensis</i> strain P2	99%	HQ432810.1	3320
EP38	<i>Bacillus</i> sp. strain Bac7	96%	KX500240.1	650
EP39	n/a	n/a	n/a	430
EP40	n/a	n/a	n/a	30
EP41	<i>Bacillus foraminis</i> strain skuast2	97%	KY548645.1	755
EP42	<i>Bacillus</i> sp. M16-1	99%	EF690408.1	2580
EP43	<i>Bacillus thuringiensis</i> strain AHL1	99%	KT456534.1	40
EN1	<i>Bacillus subtilis</i> strain BGR261	98%	KT074466.1	190
EN2	<i>Staphylococcus epidermidis</i> strain HNL22	99%	EU373364.1	878
EN3	<i>Staphylococcus</i> sp. iMSN20	99%	DQ401244.1	1147
EN4	<i>Staphylococcus epidermidis</i> strain iCTE621	99%	DQ122332.1	813
EN5	<i>Staphylococcus epidermidis</i> strain JPR-05	99%	HE716945.1	427
EN6	<i>Micrococcus aloeverae</i> strain PP-06	98%	KX082870.1	640
EN7	<i>Micrococcus luteus</i> strain LHR-04	97%	HE716930.1	348
EN8	<i>Bacillus subtilis</i> strain NB-01	99%	HM214542.1	50
EN9	<i>Bacillus pumilus</i> strain U38	99%	KC551966.1	350
EN10	<i>Micrococcus luteus</i> strain IARI-THW-25	98%	KF054946.1	160
EN11	<i>Bacillus</i> sp. IHB B 4034	99%	HM233998.1	6180
EN12	<i>Bacillus subtilis</i> subsp. <i>subtilis</i> strain RG	99%	JQ045774.1	660
EN13	<i>Bacillus pumilus</i> strain U38	99%	KC551966.1	280
EN14	<i>Acinetobacter lwooffii</i> strain CI-01	98%	KC178575.1	5665
EN15	<i>Bacillus aryabhatai</i> strain IARI-PC4-6	91%	KT149746.1	871

<sup>1</sup> EN—endophyte, EP—epiphyte; <sup>2</sup> n/a—no positive reaction.

Table A2. Primer sequences used for PCR.

Name	Sequence from 5' to 3'	Reference
27F	AGAGTTTGATCATGGCTCAG	[56]
518R	GTATTACCGCGGCTGCTGG	[56]
23S30R	CTTCGCCTCTGTGTGCCTAGGT	[57,58]
CYA359F	GGGGAATYTTCCGCAATGGG	[58,59]
nif-Df	GATTTTCADGADAADGATATT	[60]
nif-Dr	CCAIGGIATICCDTATTTTC	

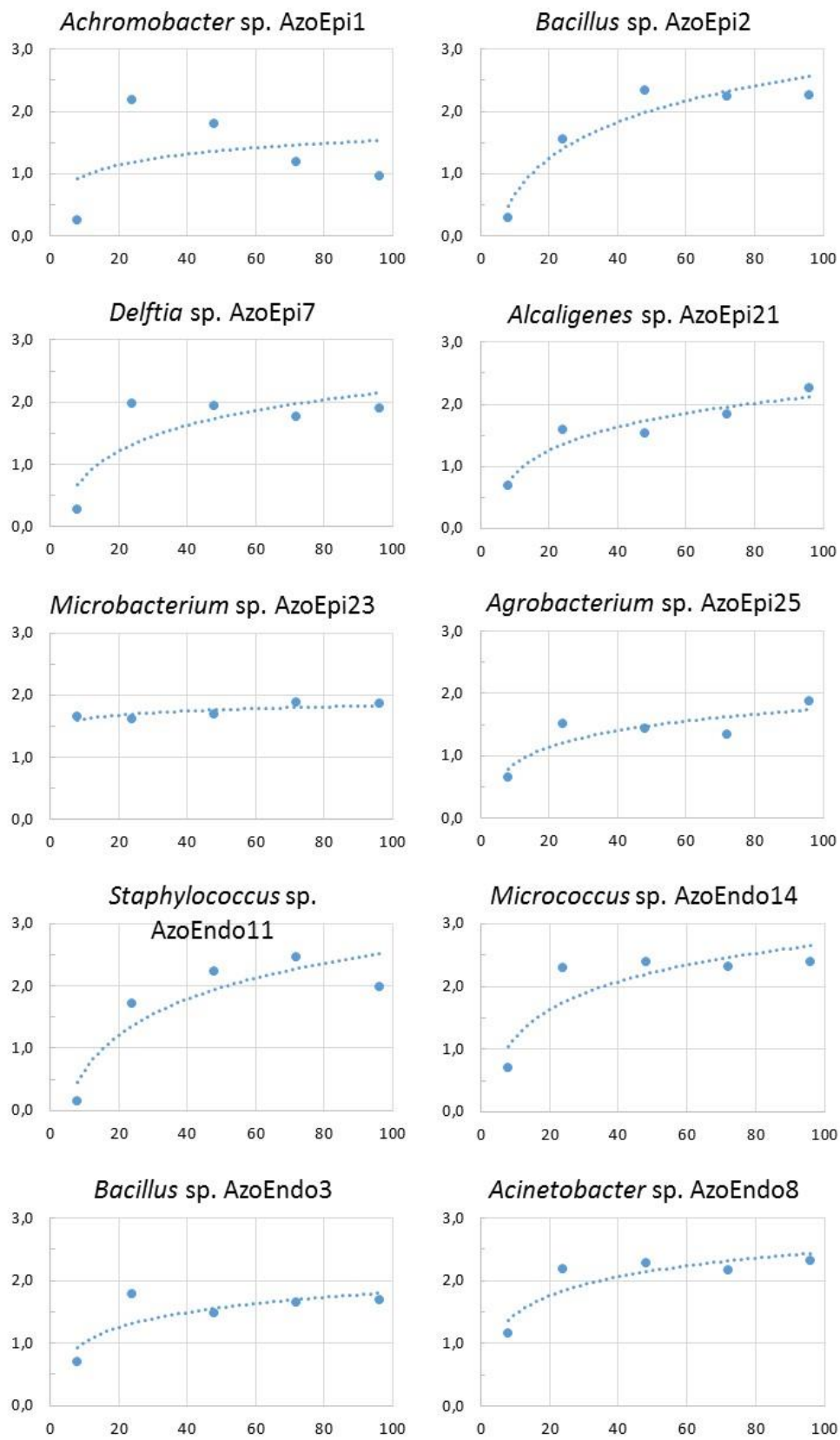


**Figure A1.** Growth curves for the cultured microorganisms selected for phenotyping. X-axis presents time of incubation (hours) and Y-axis values of OD<sub>600</sub>. Logarithmic curves are fitted to the data.

## References

1. Gdanetz, K. The wheat microbiome under four management strategies, and potential for endophytes in disease control. *Phytobiomes* **2017**, *1*, 158–168. [[CrossRef](#)]
2. Rout, M.E. The plant microbiome. In *Genomes of Herbaceous Land Plants*, 1st ed.; Paterson, A., Ed.; Academic Press: London, UK, 2014; Volume 69, pp. 279–309.
3. Hardoim, P.R.; van Overbeek, L.S.; Berg, G.; Pirttilä, A.M.; Compant, S.; Campisano, A.; Döring, M.; Sessitsch, A. The Hidden World within Plants: Ecological and Evolutionary Considerations for Defining Functioning of Microbial Endophytes. *Microbiol. Mol. Biol. Rev.* **2015**, *79*, 293–320. [[CrossRef](#)] [[PubMed](#)]
4. Berg, G.; Rybakowa, D.; Grube, M.; Köberl, M. The plant microbiome explored: Implications for experimental botany. *J. Exp. Bot.* **2016**, *67*, 995–1002. [[CrossRef](#)] [[PubMed](#)]
5. Croes, S.; Weyens, N.; Colpaert, J.; Vangronsveld, J. Characterization of the cultivable bacterial populations associated with field grown *Brassica napus* L.: An evaluation of sampling and isolation protocols. *Environ. Microbiol.* **2015**, *17*, 2379–2392. [[CrossRef](#)] [[PubMed](#)]
6. Santoyo, G.; Moreno-Hagelsieb, G.; Orozco-Mosqueda, M.C.; Glick, B.R. Plant growth-promoting bacterial endophytes. *Microbiol. Res.* **2016**, *183*, 92–99. [[CrossRef](#)] [[PubMed](#)]
7. Egamberdieva, D.; Abd-Allah, E.F.; da Silva, J.T.A. Microbially assisted phytoremediation of heavy metal-contaminated soils. In *Plant Metal Interaction. Emerging Remediation Techniques*; Parvaiz, A., Ed.; Elsevier Inc.: Amsterdam, The Netherlands, 2016; pp. 483–498.
8. Złoch, M.; Thiem, D.; Gadzała-Kopciuch, R.; Hrynkiewicz, K. Synthesis of siderophores by plant-associated metallotolerant bacteria under exposure to Cd<sup>2+</sup>. *Chemosphere* **2016**, *156*, 312–325. [[CrossRef](#)]
9. Glick, B.R. Plant Growth-Promoting Bacteria: Mechanisms and Applications. *Scientifica (Cairo)* **2012**, *2012*, 963401. [[CrossRef](#)] [[PubMed](#)]
10. Carrapiço, F. Azolla as a Superorganism. Its Implication in Symbiotic Studies. In *Symbioses and Stress. Cellular Origin, Life in Extreme Habitats and Astrobiology*; Seckbach, J., Grube, M., Eds.; Springer: Dordrecht, The Netherlands, 2010; Volume 17, pp. 225–241.
11. Banach, A.M.; Banach, K.; Stepniewska, Z. Phytoremediation as a promising technology for water and soil purification: *Azolla caroliniana* Willd. As a case study. *Acta Agrophysica* **2012**, *19*, 241–252.
12. Sood, A.; Uniyal, P.L.; Prasanna, R.; Ahluwalia, A.S. Phytoremediation Potential of Aquatic Macrophyte, *Azolla*. *Ambio* **2012**, *41*, 122–137. [[CrossRef](#)] [[PubMed](#)]
13. Plazinski, J.; Zheng, Q.; Taylor, R.; Croft, L.; Rolfe, B.G.; Gunning, B.E.S. DNA probes show genetic variation in cyanobacterial symbionts of the *Azolla* fern and a closer relationship to free-living *Nostoc* strains than to free-living *Anabaena* strains. *Appl. Environ. Microbiol.* **1990**, *56*, 1263–1270.
14. Gebhardt, J.S.; Nierzwicki-Bauer, S.A. Identification of a common cyanobacterial symbiont associated with *Azolla* spp. through molecular and morphological characterization of free-living and symbiotic cyanobacteria. *Appl. Environ. Microbiol.* **1991**, *57*, 2141–2146. [[PubMed](#)]
15. Baker, J.A.; Entsch, B.; McKay, D.B. The cyanobiont in an *Azolla* fern is neither *Anabaena* nor *Nostoc*. *FEMS Microbiol. Lett.* **2003**, *229*, 43–47. [[CrossRef](#)]
16. Pereira, A.L.; Vasconcelos, V. Classification and phylogeny of the cyanobiont *Anabaena azollae* Strasburger: An answered question? *Int. J. Syst. Evol. Microbiol.* **2014**, *64*, 1830–1840. [[CrossRef](#)] [[PubMed](#)]
17. Grilli, M. Infrastrutture di *Anabaena azollae* vivente nelle foglioline di *Azolla caroliniana* (in Italian). *Ann. Microb. Enzim* **1964**, *XIV*, 69–90.
18. Nierzwicki-Bauer, S.A.; Aulfinger, H. Occurrence and Ultrastructural Characterization of Bacteria in Association with and Isolated from *Azolla caroliniana*. *Appl. Environ. Microb.* **1991**, *57*, 3629–3636.
19. Carrapiço, F. Are bacteria the third partner of the *Azolla-Anabaena* symbiosis? *Plant Soil* **1991**, *137*, 157–160. [[CrossRef](#)]
20. Serrano, R.; Carrapiço, F.; Vidal, R. The Presence of Lectins in Bacteria Associated with the *Azolla-Anabaena* Symbiosis. *Symbiosis* **1999**, *27*, 169–178.
21. Zagajewski, P. Influence of environmental factors on growth and toxin production by cyanobacterial species (in Polish). Ph.D. Thesis, Adam Mickiewicz University Poznań. Faculty of Biology, Department of Water Protection, Poznań, Poland, 2012; pp. 64–65.

22. Kozlikova-Zapomelova, E.; Chatchawan, T.; Kastovsky, J.; Komárek, J. Phylogenetic and taxonomic position of the genus *Wollea* with the description of *Wollea salina* sp. nov. (Cyanobacteria, Nostocales). *Fottea* **2016**, *16*, 43–55. [CrossRef]
23. Shishido, J.; Humisto, A.; Jokela, J.; Liu, L.; Wahlsten, M.; Tamrakar, A.; Fewer, D.P.; Permi, P.; Andreote, A.P.; Fiore, M.F.; et al. Antifungal compounds from cyanobacteria. *Mar. Drugs* **2015**, *13*, 2124–2140. [CrossRef] [PubMed]
24. Gugger, M.; Lyra, C.; Henriksen, P.; Couté, A.; Humbert, J.-F.; Sivonen, K. Phylogenetic comparison of the cyanobacterial genera *Anabaena* and *Aphanizomenon*. *Int. J. Syst. Evol. Microbiol.* **2002**, *52*, 1867–1880. [CrossRef]
25. Willame, R.; Boutte, C.; Grubisic, S.; Wilmotte, A.; Komárek, J.; Hoffmann, L. Morphological and molecular characterization of planktonic cyanobacteria from Belgium and Luxembourg. *J. Phycol.* **2006**, *42*, 1312–1332. [CrossRef]
26. Dijkhuizen, L.W.; Brouwer, P.; Bolhuis, H.; Reichart, G.-J.; Koppers, N.; Huettel, B.; Bolger, A.M.; Li, F.W.; Cheng, S.; Liu, X.; et al. Is there foul play in the leaf pocket? The metagenome of floating fern *Azolla* reveals endophytes that do not fix N<sub>2</sub> but may denitrify. *New Phytol.* **2018**, *217*, 453–466. [CrossRef] [PubMed]
27. Komárek, J.; Anagnostidis, K. Modern approach to the classification system of cyanophytes. *Nostocales. Arch. Hydrobiol. Suppl. Algal. Stud.* **1989**, *56*, 247–345.
28. Canter-Lund, H.; Lund, J.W.G. *Freshwater Algae: Their Microscopic World Explored*; Biopress Ltd.: Bristol, UK, 1995; p. 360.
29. Guiry, M.D.; Guiry, G.M. *AlgaeBase*. World-wide electronic publication, National University of Ireland, Galway. Available online: [http://www.algaebase.org/search/species/detail/?species\\_id=65456](http://www.algaebase.org/search/species/detail/?species_id=65456) (accessed on 15 April 2019).
30. Forni, C.; Riov, J.; Caiola, M.G.; Tel-Or, E. Indole-3-acetic acid (IAA) production by *Arthrobacter* species isolated from *Azolla*. *J. Gen. Microbiol.* **1992**, *138*, 377–381. [CrossRef] [PubMed]
31. Ghodsavali, B.; Ahmadzadeh, M.; Soleimani, M.; Madloo, P.B.; Taghizad-Farid, R. Isolation and characterization of rhizobacteria and their effects on root extracts of *Valeriana officinalis*. *Aust. J. Crop Sci.* **2013**, *7*, 338–344.
32. Dutta, J.; Handique, P.J.; Thakur, D. Assessment of Culturable Tea Rhizobacteria Isolated from Tea Estates of Assam, India for Growth Promotion in Commercial Tea Cultivars. *Front. Microbiol.* **2015**, *6*, 1252. [CrossRef] [PubMed]
33. Morel, M.; Iriarte, A.; Jara, E.; Musto, H.; Castro-Sowinski, S. Revealing the biotechnological potential of *Delftia* sp. JD2 by a genomic approach. *AIMS Bioeng* **2016**, *3*, 156–175. [CrossRef]
34. Cho, K.M.; Hong, S.Y.; Lee, S.M.; Kim, Y.H.; Kahng, G.G.; Lim, Y.P.; Kim, H.; Yun, H.D. Endophytic Bacterial Communities in Ginseng and their Antifungal Activity Against Pathogens. *Microb. Ecol.* **2007**, *54*, 341–351. [CrossRef]
35. Jorquera, M.A.; Hernández, M.T.; Rengel, Z.; Marschner, P.; de la Luz Mora, M. Isolation of culturable phosphobacteria with both phytate-mineralization and phosphate-solubilization activity from the rhizosphere of plants grown in a volcanic soil. *Biol. Fertil. Soils* **2008**, *44*, 1025–1034. [CrossRef]
36. Chen, Y.P.; Rekha, P.D.; Arun, A.B.; Shen, F.T.; Lai, W.-A.; Young, C.C. Phosphate solubilizing bacteria from subtropical soil and their tricalcium phosphate solubilizing abilities. *Appl. Soil. Ecol.* **2006**, *34*, 33–41. [CrossRef]
37. Liu, Y.; Tie, B.; Li, Y.; Lei, M.; Wei, X.; Liu, X.; Du, H. Inoculation of soil with cadmium-resistant bacterium *Delftia* sp. B9 reduces cadmium accumulation in rice (*Oryza sativa* L.) grains. *Ecotoxicol. Environ. Saf.* **2018**, *163*, 223–229. [CrossRef] [PubMed]
38. Xu, X.; Liu, W.; Wang, W.; Tian, S.; Jiang, P.; Qi, Q.; Li, F.; Li, H.; Wang, Q.; Li, H.; Yu, H. Potential biodegradation of phenanthrene by isolated halotolerant bacterial strains from petroleum oil polluted soil in Yellow River Delta. *Sci Total Environ* **2019**, *664*, 1030–1038. [CrossRef] [PubMed]
39. Braña, V.; Cagide, C.; Morel, M.A. The sustainable use of *Delftia* in agriculture, bioremediation, and bioproducts synthesis. In *Microbial Models: From Environmental to Industrial Sustainability*, 1st ed.; Castro-Sowinski, S., Ed.; Springer: Singapore, 2016; pp. 227–247.
40. Wu, W.; Huang, H.; Ling, Z.; Yu, Z.; Jaing, Y.; Liu, P.; Li, X. Genome sequencing reveals mechanisms for heavy metal resistance and polycyclic aromatic hydrocarbon degradation in *Delftia lacustris* strain LZ-C. *Ecotoxicology* **2016**, *25*, 234–247. [CrossRef]

41. Hou, Q.; Wang, C.; Guo, H.; Xia, Z.; Ye, J.; Liu, K.; Yang, Y.; Hou, X.; Liu, H.; Wang, J.; Du, B.; Ding, Y. Draft genome sequence of *Delftia tsuruhatensis* MTQ3, a strain of plant growth-promoting rhizobacterium with antimicrobial activity. *Genome Announc* **2015**, *3*, e00822-15. [[CrossRef](#)]
42. Johnston, C.W.; Wyatt, M.A.; Li, X.; Ibrahim, A.; Shuster, J.; Southam, G.; Magarvey, N.A. Gold biomineralization by a metallophore from a gold-associated microbe. *Nat. Chem. Biol.* **2013**, *9*, 241–243. [[CrossRef](#)]
43. Li, G.-X.; Zhou, S.-Y.-D.; Ren, H.-Y.; Xue, X.-M.; Xu, Y.-Y.; Bao, P. Extracellular Biomineralization of Gold by *Delftia tsuruhatensis* GX-3 Isolated from a Heavy Metal Contaminated Paddy Soil. *ACS Earth Space Chem* **2018**, *2*, 1294–1300. [[CrossRef](#)]
44. Jangir, Y.; French, S.; Momper, L.M.; Moser, D.P.; Amend, J.P.; El-Naggar, M.Y. Isolation and Characterization of Electrochemically Active Subsurface *Delftia* and *Azonexus* Species. *Front Microbiol* **2016**, *7*, 756. [[CrossRef](#)] [[PubMed](#)]
45. Shetty, A.; Chen, S.; Tocheva, E.I.; Jensen, G.J.; Hickey, W.J. Nanopods: A New Bacterial Structure and Mechanism for Deployment of Outer Membrane Vesicles. *PLoS ONE* **2011**, *6*, e20725. [[CrossRef](#)] [[PubMed](#)]
46. Ahemad, M. Phosphate-solubilizing bacteria-assisted phytoremediation of metalliferous soils: A review. *3 Biotech* **2015**, *5*, 111–121. [[CrossRef](#)]
47. Watanabe, I.; Roger, P.A.; Ladha, J.K.; Van Hove, C. *Biofertilizer germplasm collections at IRRI*; International Rice Research Institute: Manila, Philippines, 1992; p. 8.
48. Komárek, J. Cyanoprokaryota: 3rd Part: Heterocystous Genera. In *Süßwasserflora von Mitteleuropa*; Büdel, B., Gärtner, G., Krienitz, L., Schagerl, M., Eds.; Springer Spektrum: Berlin/Heidelberg, Germany, 2013; Volume 19, pp. 1–1130.
49. Hindák, F. *Fotografický atlas mikroskopických sinic (in Slovak)*; VEDA: Bratislava, Slovakia, 2001; p. 257.
50. Stepniewska, Z.; Goraj, W.; Kuźniar, A.; Łopacka, N.; Małyszka, M. Enrichment culture and identification of endophytic methanotrophs isolated from peatland plants. *Folia Microbiol.* **2017**, *62*, 381–391. [[CrossRef](#)]
51. Truyens, S.; Weyens, S.; Cuypers, A.; Vangronsveld, J. Changes in the population of seed bacteria of transgenerationally Cd-exposed *Arabidopsis thaliana*. *Plant Biol. (Stuttg)* **2013**, *15*, 971–981. [[CrossRef](#)]
52. Kasana, R.C.; Salwan, R.; Dhar, H.; Dutt, S.; Gulati, A. A Rapid and Easy Method for the Detection of Microbial Cellulases on Agar Plates Using Gram's Iodine. *Curr. Microbiol.* **2008**, *57*, 503–507. [[CrossRef](#)]
53. Alexander, D.B.; Zuberer, D.A. Use of chrome azurol S reagents to evaluate siderophore production by rhizosphere bacteria. *Biol Fertil Soils* **1991**, *12*, 39–45. [[CrossRef](#)]
54. Sambrook, J.; Russell, R.W. *Molecular cloning: A laboratory manual*, 3rd ed.; Cold Spring Harbor Laboratory Press: New York, NY, USA, 2001; p. 2100.
55. Gordon, S.; Weber, R. Colorimetric estimation of indoleacetic acid. *Plant Physiol.* **1951**, *26*, 192–195. [[CrossRef](#)] [[PubMed](#)]
56. Lee, T.K.; Doan, T.V.; Yoo, K.; Choi, S.; Kim, C.; Park, J. Discovery of commonly existing anode biofilm microbes in two different wastewater treatment MFCs using FLX Titanium pyrosequencing. *Appl. Microbiol. Biotechnol.* **2010**, *87*, 2335–2343. [[CrossRef](#)] [[PubMed](#)]
57. Taton, A.; Grubisic, S.; Brambilla, E.; De Wit, R.; Wilmotte, A. Cyanobacterial Diversity in Natural and Artificial Microbial Mats of Lake Fryxell (McMurdo Dry Valleys, Antarctica): A Morphological and Molecular Approach. *Appl. Microbiol. Biotechnol.* **2003**, *69*, 5157–5169. [[CrossRef](#)]
58. Koskenniemi, K.; Lyra, Ch.; Rajaniemi-Wacklin, P.; Jokela, J.; Sivonen, K. Quantitative Real-Time PCR Detection of Toxic *Nodularia* Cyanobacteria in the Baltic Sea. *Appl. Environ. Microb.* **2007**, *73*, 2173–2179. [[CrossRef](#)]
59. Nübel, U.; Garcia-Pichel, F.; Muyzer, G. PCR Primers To Amplify 16S rRNA Genes from Cyanobacteria. *Appl. Environ. Microb.* **1997**, *63*, 3327–3332.
60. Dedysh, S.; Ricke, P.; Liesack, W. NifH and NifD phylogenies: An evolutionary basis for understanding nitrogen fixation capabilities of methanotrophic bacteria. *Microbiology* **2004**, *150*, 1301–1313. [[CrossRef](#)]

